Article

Chinese Science Bulletin

Quantum Information

October 2013 Vol. 58 No. 28-29: 3507–3513
doi: 10.1007/s11434-013-6019-4

Multipartite entanglement concentration for nitrogen-vacancy center and microtoroidal resonator system

SHENG YuBo[1,2], LIU Jiong[1,2], ZHAO ShengYang[1,2] & ZHOU Lan[1,3*]

[1] *Key Laboratory of Broadband Wireless Communication and Sensor Network Technology, Nanjing University of Posts and Telecommunications, Ministry of Education, Nanjing 210003, China;*
[2] *Institute of Signal Processing Transmission, Nanjing University of Posts and Telecommunications, Nanjing 210003, China;*
[3] *College of Mathematics and Physics, Nanjing University of Posts and Telecommunications, Nanjing 210003, China*

Received January 19, 2013; accepted May 17, 2013

We describe a high efficient entanglement concentration protocol (ECP) for multi-particle less-entangled nitrogen-vacancy (N-V) center and microtoroidal resonator system. In the ECP, we only require one pair of less-entangled state, two auxiliary N-V center in microcavities and some single photons. After the photon passing through the microcavity, by measuring the polarization of the photon, a maximally entangled W state can be obtained with some success probability. This ECP does not need to destroy the solid qubit, which makes it more feasible. Moreover, by resorting to more single photons, it can be repeated to reach a high success probability. These features make this ECP useful in current long-distance quantum communications.

quantum communication, entanglement, entanglement concentration, nitrogen-vacancy center, decoherence

Citation: Sheng Y B, Liu J, Zhao S Y, et al. Multipartite entanglement concentration for nitrogen-vacancy center and microtoroidal resonator system. Chin Sci Bull, 2013, 58: 3507–3513, doi: 10.1007/s11434-013-6019-4

Quantum communication deals with the transmission and exchange of quantum information between distant nodes of a network [1]. Such transmission and exchange of quantum information has potential application in the secret transfer of classical messages by means of quantum key distribution [2–5], teleportation [6–8], quantum denescoding [9–11], quantum secret sharing [12–14], quantum state sharing [15–17], quantum secure direct communication [18–22], and other protocols [23–27]. The basic principle of quantum communication is to generate nearly perfect entangled states between distant locations. Quantum repeaters are used to extend the length of quantum channel, which is used to resist the photon loss. On the other hand, the perfect entangled state will also be degraded because of the environment noise. The maximally entangled state will become a mixed state or a less-entangled states.

Entanglement purification is to distill some high quality entangled states from a large ensembles of low quality entangled states, which has been widely studied [28–35]. Entanglement concentration is to recover some maximally entangled states from a large ensembles of pure less-entangled ensembles [36–64]. In 1996, Bennett et al. [36] described an entanglement concentration protocol (ECP) with collective measurement. The ECP with entanglement swapping was developed by Shi et al. [37]. The ECPs with linear optics were proposed in 2001 [38, 39]. These protocols were developed in 2008 with the help of cross-Kerr nonlinearity [40–42]. Most of the ECPs focused on the photons [38–44, 46–51]. During the past few years, the ECPs for solid entangled systems were also proposed, such as the ECP for quantum dot and microcavity coupling system [54, 55], electrons [56–58], atoms [59] and so on [62–65].

Recently, the nitrogen-vacancy (N-V) defect center in diamond becomes a promising candidate for solid quantum information processing. The N-V centers are negatively charged with six electrons from the nitrogen [66, 67]. The vacancy are surrounded by three carbons. A lot of theoretical and experimental works have been devoted into such systems, for it provides us enough lifetime to manipulate at room temperature. In 2010, Yang et al. [68] discussed the entangle-

*Corresponding author (email: zhoul@njupt.edu.cn)

ment of separate N-V centers coupled to a whispering-gallery mode cavity. In their paper, they presented the W-state and Bell-state entanglement generation using N-V centers coupled to whispering-gallery mode cavity. They also showed that the N-V center ensemble is the high-fidelity quantum memory for quantum computation [69]. In 2011, Chen et al. [70] proposed a practical scheme to entangle negatively charged N-V centers in distant diamonds. Li et al. [71] also discussed the quantum-information transfer with N-V centers coupled to a whispering-gallery microresonator. Jiang et al. [72] reported their experiment result for repetitive readout of a single electronic spin via quantum logic with nuclear spin ancillae. The entanglement between an optical photon and a solid-state spin qubit was also realized. In 2012, the entanglement purification protocol for N-V centers via coupling to microtoroidal resonators was proposed [73].

Inspired by the excellent works of entanglement concentration and quantum information processing based on the N-V centers, in this paper, we present an implementation of ECP for multi-particle entangled N-V centers via the coupled with microtoroidal resonators. We resort two single N-V centers and two single photons to complete the task. After performing the ECP, one can obtain the maximally entangled W states with some success probability. During the process, we do not need to destroy the solid qubits. Moreover, the ECP can be repeated to obtain a high success probability. These advantages make it useful in current long-distance communication.

1 Basic model of the ECP

In this section, we will briefly describe the model that a single N-V center is coupled by the evanescent field of the microtoroidal resonator, which can be described as a double-side optical cavity. In this model, the N-V center can be regarded as an additional electron with a negative charge that consists of a substitutional nitrogen atom and an adjacent vacancy. The ground state is a spin triplet with the splitting at 2.87 GHz between levels $|g_0\rangle$ ($m_s = 0$) and $|g_{\pm1}\rangle$ ($m_s = \pm1$) owing to spin-spin interactions. The six excited states are defined by group theory as shown in [67]. In Figure 1, one of the excited state $|A_2\rangle$ can be described as $|A_2\rangle = |E_-\rangle|g_{+1}\rangle + |E_+\rangle|g_{-1}\rangle$. Here $|E_\pm\rangle$ are orbital states. The possible cavity-mode-induced transitions are $|g_{-1}\rangle \leftrightarrow |A_2\rangle$ and $|g_{+1}\rangle \leftrightarrow |A_2\rangle$ by absorbing and emitting an $|L\rangle$ and $|R\rangle$ circularly polarized photon, respectively. We make a single-photon pulse with frequency ω_p enter a microresonator cavity with the mode frequency ω_c. Such coupled system essentially exhibits similar features with the Jaynes-Cummings model. The adiabatical elimination of the cavity mode leads to the reflection coefficient as [70]

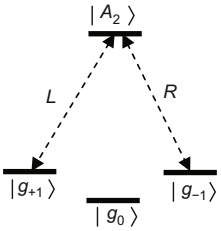

Figure 1 The N-V center couples to microtoroidal cavity. The $|g_{\pm1}\rangle$ are two generated states which couple with left $|L\rangle$ and right $|R\rangle$ polarization photon, respectively. The $|g_0\rangle$ is the ground state. The quantum qubits are encoded in $|g_{\pm1}\rangle$.

$$r(\omega) = \frac{[i(\omega_c - \omega_p) - \frac{\kappa}{2}][i(\omega_0 - \omega_p) + \frac{\gamma}{2}] + \Omega^2}{[i(\omega_c - \omega_p) + \frac{\kappa}{2}][i(\omega_0 - \omega_p) + \frac{\gamma}{2}] + \Omega^2}. \quad (1)$$

The ω_0 is the transition frequency between $|A_2\rangle$ and $|g_{-1}\rangle$. The γ and κ are the N-V center dipolar decay rate and the cavity damping rate, respectively. Ω means the term for the coupling of the N-V center to the cavity. From eq. (1), on the resonant condition of the system with $\omega_0 = \omega_c = \omega_p$ and $\Omega = 0$, above equation for an empty cavity can be written as [70, 73]

$$r_0(\omega) = \frac{i(\omega_c - \omega_p) - \frac{\kappa}{2}}{i(\omega_c - \omega_p) + \frac{\kappa}{2}}. \quad (2)$$

Therefore, if the initial state is $|g_{-1}\rangle$ and the photon is $|L\rangle$, the output photon pulse will be driven as $|L\rangle \rightarrow r(\omega)|L\rangle = e^{i\theta}|L\rangle$. Here the phase θ is the phase shift determined by the input-output relation. On the other hand, if the initial photon is prepared in the $|R\rangle$ state, it will become $|R\rangle \rightarrow r_0(\omega)|R\rangle = e^{i\theta_0}|R\rangle$. The θ_0 is the reflection coefficient from eq. (2). If the initial state is $|g_{+1}\rangle$ and the photon is $|L\rangle$, the output photon will evolve as $|L\rangle \rightarrow r(\omega_0)|L\rangle = e^{i\theta_0}|L\rangle$ and the $|R\rangle$ photon will evolve as $|R\rangle \rightarrow r(\omega)|R\rangle = e^{i\theta}|R\rangle$.

If we consider a special case that the $\theta_0 = \frac{\pi}{2}$ and $\theta = 0$, the above relationship can be regarded as the parity check measurement (PCM) for N-V center spins. If the photon passes through two N-V center spins, the input-output relationship can be written as

$$\begin{aligned}
&\frac{|L\rangle + |R\rangle}{\sqrt{2}}|g_{+1}\rangle|g_{+1}\rangle \rightarrow \frac{|L\rangle - |R\rangle}{\sqrt{2}}|g_{+1}\rangle|g_{+1}\rangle,\\
&\frac{|L\rangle + |R\rangle}{\sqrt{2}}|g_{-1}\rangle|g_{-1}\rangle \rightarrow \frac{|L\rangle - |R\rangle}{\sqrt{2}}|g_{-1}\rangle|g_{-1}\rangle,\\
&\frac{|L\rangle + |R\rangle}{\sqrt{2}}|g_{+1}\rangle|g_{-1}\rangle \rightarrow \frac{|L\rangle + |R\rangle}{\sqrt{2}}|g_{+1}\rangle|g_{-1}\rangle,\\
&\frac{|L\rangle + |R\rangle}{\sqrt{2}}|g_{-1}\rangle|g_{+1}\rangle \rightarrow \frac{|L\rangle + |R\rangle}{\sqrt{2}}|g_{-1}\rangle|g_{+1}\rangle.
\end{aligned} \quad (3)$$

In this way, the even parity state $|g_{+1}\rangle|g_{+1}\rangle$ and $|g_{-1}\rangle|g_{-1}\rangle$ can be easily distinguished from the odd parity state $|g_{+1}\rangle|g_{-1}\rangle$ and $|g_{-1}\rangle|g_{+1}\rangle$ according to the different polarization of the photon. The state $\frac{|L\rangle - |R\rangle}{\sqrt{2}}$ and $\frac{|L\rangle + |R\rangle}{\sqrt{2}}$ are two orthogonal states which can be distinguished by their spatial mode after passing through the polarization beam splitter (PBS).

2 ECP on N-V centers coupled to microtoroidal resonators

From Figure 2, we suppose the three parities, say Alice, Bob and Charlie, share the three-particle less-entangled state

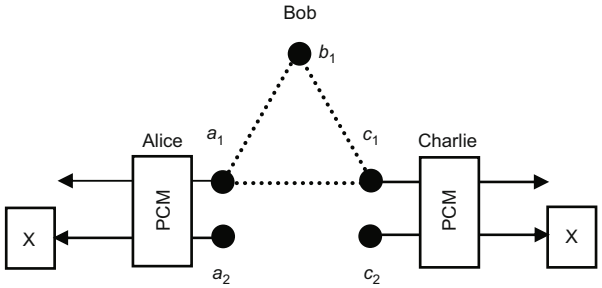

Figure 2 Schematic diagram showing the basic principle of our ECP for entangled N-V centers. PCM is the parity check measurement which is performed by single photons. The X indicates the measurement in the basis $|\pm x\rangle = \frac{1}{\sqrt{2}}(|g_{+1}\rangle \pm |g_{-1}\rangle)$.

$|\Phi\rangle_{a_1b_1c_1}$, which can be described as

$$\begin{aligned}|\Phi\rangle_{a_1b_1c_1} = {} & \alpha|g_{-1}\rangle_{a_1}|g_{+1}\rangle_{b_1}|g_{+1}\rangle_{c_1} \\ & + \beta|g_{+1}\rangle_{a_1}|g_{-1}\rangle_{b_1}|g_{+1}\rangle_{c_1} \\ & + \delta|g_{+1}\rangle_{a_1}|g_{+1}\rangle_{b_1}|g_{-1}\rangle_{c_1}. \end{aligned} \tag{4}$$

Alice first prepares an ancillary N-V center a_2 in the following state

$$|\Phi\rangle_{a_2} = \frac{\alpha}{\sqrt{\alpha^2+\beta^2}}|g_{+1}\rangle_{a_2} + \frac{\beta}{\sqrt{\alpha^2+\beta^2}}|g_{-1}\rangle_{a_2}. \tag{5}$$

Alice also prepares a single photon state of the form $|\Phi\rangle_p = \frac{1}{\sqrt{2}}(|L\rangle + |R\rangle)$. Here $|\alpha|^2 + |\beta|^2 + |\delta|^2 = 1$. The whole system can be written as

$$\begin{aligned}|\Phi\rangle_{a_1b_1c_1} \otimes |\Phi\rangle_{a_2} = {} & (\alpha|g_{-1}\rangle_{a_1}|g_{+1}\rangle_{b_1}|g_{+1}\rangle_{c_1} \\ & + \beta|g_{+1}\rangle_{a_1}|g_{-1}\rangle_{b_1}|g_{+1}\rangle_{c_1} \\ & + \delta|g_{+1}\rangle_{a_1}|g_{+1}\rangle_{b_1}|g_{-1}\rangle_{c_1}) \\ & \otimes \left(\frac{\alpha}{\sqrt{\alpha^2+\beta^2}}|g_{+1}\rangle_{a_2} + \frac{\beta}{\sqrt{\alpha^2+\beta^2}}|g_{-1}\rangle_{a_2}\right) \\ = {} & \frac{\alpha^2}{\sqrt{\alpha^2+\beta^2}}|g_{-1}\rangle_{a_1}|g_{+1}\rangle_{a_2}|g_{+1}\rangle_{b_1}|g_{+1}\rangle_{c_1} \\ & + \frac{\beta^2}{\sqrt{\alpha^2+\beta^2}}|g_{+1}\rangle_{a_1}|g_{-1}\rangle_{a2}|g_{-1}\rangle_{b1}|g_{+1}\rangle_{c1} \\ & + \frac{\alpha\delta}{\sqrt{\alpha^2+\beta^2}}|g_{+1}\rangle_{a_1}|g_{+1}\rangle_{a_2}|g_{+1}\rangle_{b_1}|g_{-1}\rangle_{c_1} \\ & + \frac{\beta\delta}{\sqrt{\alpha^2+\beta^2}}|g_{+1}\rangle_{a_1}|g_{-1}\rangle_{a_2}|g_{+1}\rangle_{b_1}|g_{-1}\rangle_{c_1} \\ & + \frac{\alpha\beta}{\sqrt{\alpha^2+\beta^2}}|g_{-1}\rangle_{a_1}|g_{-1}\rangle_{a_2}|g_{+1}\rangle_{b_1}|g_{+1}\rangle_{c_1} \\ & + \frac{\alpha\beta}{\sqrt{\alpha^2+\beta^2}}|g_{+1}\rangle_{a_1}|g_{+1}\rangle_{a_2}|g_{-1}\rangle_{b_1}|g_{+1}\rangle_{c_1}. \end{aligned} \tag{6}$$

From eq. (6), it can be found that the items $|g_{+1}\rangle_{a_1}|g_{+1}\rangle_{a_2}|g_{+1}\rangle_{b_1}|g_{-1}\rangle_{c_1}$, $|g_{-1}\rangle_{a_1}|g_{-1}\rangle_{a_2}|g_{+1}\rangle_{b_1}|g_{+1}\rangle_{c_1}$ and $|g_{+1}\rangle_{a_1}|g_{+1}\rangle_{a_2}|g_{-1}\rangle_{b_1}|g_{+1}\rangle_{c_1}$ will make the polarization of the photon flip to $\frac{1}{\sqrt{2}}(|L\rangle - |R\rangle)$. Therefore, if the photon is flipped which can be detected by the single-photon detector, they can obtain

$$\begin{aligned}|\Psi\rangle' = {} & \frac{\alpha\delta}{\sqrt{\alpha^2+\beta^2}}|g_{+1}\rangle_{a_1}|g_{+1}\rangle_{a_2}|g_{+1}\rangle_{b_1}|g_{-1}\rangle_{c_1} \\ & + \frac{\alpha\beta}{\sqrt{\alpha^2+\beta^2}}|g_{-1}\rangle_{a_1}|g_{-1}\rangle_{a_2}|g_{+1}\rangle_{b_1}|g_{+1}\rangle_{c_1} \\ & + \frac{\alpha\beta}{\sqrt{\alpha^2+\beta^2}}|g_{+1}\rangle_{a_1}|g_{+1}\rangle_{a_2}|g_{-1}\rangle_{b_1}|g_{+1}\rangle_{c_1}, \end{aligned} \tag{7}$$

with a success probability of

$$P^1 = \frac{|\alpha|^2(|\delta|^2 + 2|\beta|^2)}{|\alpha|^2 + |\beta|^2}. \tag{8}$$

Then they measure the a_2 state in the bases X as shown in Figure 2. The basis X is $|\pm x\rangle = \frac{1}{\sqrt{2}}(|g_{+1}\rangle \pm |g_{-1}\rangle)$. If the measurement result is $|+x\rangle$, they will obtain

$$\begin{aligned}|\Phi_1\rangle = {} & \frac{\delta}{\sqrt{\delta^2+2\beta^2}}|g_{+1}\rangle_{a_1}|g_{+1}\rangle_{b_1}|g_{-1}\rangle_{c_1} \\ & + \frac{\beta}{\sqrt{\delta^2+2\beta^2}}|g_{-1}\rangle_{a_1}|g_{+1}\rangle_{b_1}|g_{+1}\rangle_{c_1} \\ & + \frac{\beta}{\sqrt{\delta^2+2\beta^2}}|g_{+1}\rangle_{a_1}|g_{-1}\rangle_{b_1}|g_{+1}\rangle_{c_1}. \end{aligned} \tag{9}$$

Otherwise, if the measurement result is $|-x\rangle$, they will obtain

$$\begin{aligned}|\Phi_2\rangle = {} & \frac{\delta}{\sqrt{\delta^2+2\beta^2}}|g_{+1}\rangle_{a_1}|g_{+1}\rangle_{b_1}|g_{-1}\rangle_{c_1} \\ & - \frac{\beta}{\sqrt{\delta^2+2\beta^2}}|g_{-1}\rangle_{a_1}|g_{+1}\rangle_{b_1}|g_{+1}\rangle_{c_1} \\ & + \frac{\beta}{\sqrt{\delta^2+2\beta^2}}|g_{+1}\rangle_{a_1}|g_{-1}\rangle_{b_1}|g_{+1}\rangle_{c_1}. \end{aligned} \tag{10}$$

If they obtain the state $|\Phi_2\rangle$, they only need to perform a phase flip operation to convert it to $|\Phi_1\rangle$.

The second step for Charlie is similar to Alice. Charlie first prepares a single photon $\frac{1}{\sqrt{2}}(|L\rangle + |R\rangle)$ and another single N-V center qubit of the form

$$|\Phi\rangle_{c_2} = \frac{\beta}{\sqrt{\gamma^2+\beta^2}}|g_{-1}\rangle_{c_2} + \frac{\delta}{\sqrt{\gamma^2+\beta^2}}|g_{+1}\rangle_{c_2}. \tag{11}$$

The single N-V center qubit combined with $|\Phi_1\rangle$ can be written as

$$\begin{aligned}|\Phi_1\rangle \otimes |\Phi\rangle_{c_2} = {} & \left(\frac{\delta}{\sqrt{\delta^2+2\beta^2}}|g_{+1}\rangle_{a_1}|g_{+1}\rangle_{b_1}|g_{-1}\rangle_{c_1}\right. \\ & + \frac{\beta}{\sqrt{\delta^2+2\beta^2}}|g_{-1}\rangle_{a_1}|g_{+1}\rangle_{b_1}|g_{+1}\rangle_{c_1} \\ & \left. + \frac{\beta}{\sqrt{\delta^2+2\beta^2}}|g_{+1}\rangle_{a_1}|g_{-1}\rangle_{b_1}|g_{+1}\rangle_{c_1}\right) \\ & \otimes \left(\frac{\beta}{\sqrt{\gamma^2+\beta^2}}|g_{-1}\rangle_{c_2} + \frac{\delta}{\sqrt{\gamma^2+\beta^2}}|g_{+1}\rangle_{c_2}\right) \\ = {} & \frac{\delta}{\sqrt{\delta^2+2\beta^2}}\frac{\beta}{\sqrt{\gamma^2+\beta^2}}|g_{+1}\rangle_{a_1}|g_{+1}\rangle_{b_1}|g_{-1}\rangle_{c_1}|g_{-1}\rangle_{c_2} \end{aligned}$$

$$+\frac{\delta}{\sqrt{\delta^2+2\beta^2}}\frac{\beta}{\sqrt{\gamma^2+\beta^2}}|g_{-1}\rangle_{a_1}|g_{+1}\rangle_{b_1}|g_{+1}\rangle_{c_1}|g_{+1}\rangle_{c_2}$$
$$+\frac{\delta}{\sqrt{\delta^2+2\beta^2}}\frac{\beta}{\sqrt{\gamma^2+\beta^2}}|g_{+1}\rangle_{a_1}|g_{-1}\rangle_{b_1}|g_{+1}\rangle_{c_1}|g_{+1}\rangle_{c_2}$$
$$+\frac{\delta}{\sqrt{\delta^2+2\beta^2}}\frac{\delta}{\sqrt{\gamma^2+\beta^2}}|g_{+1}\rangle_{a_1}|g_{+1}\rangle_{b_1}|g_{-1}\rangle_{c_1}|g_{+1}\rangle_{c_2}$$
$$+\frac{\beta}{\sqrt{\delta^2+2\beta^2}}\frac{\beta}{\sqrt{\gamma^2+\beta^2}}|g_{-1}\rangle_{a_1}|g_{+1}\rangle_{b_1}|g_{+1}\rangle_{c_1}|g_{-1}\rangle_{c_2}$$
$$+\frac{\beta}{\sqrt{\delta^2+2\beta^2}}\frac{\beta}{\sqrt{\gamma^2+\beta^2}}|g_{+1}\rangle_{a_1}|g_{-1}\rangle_{b_1}|g_{+1}\rangle_{c_1}|g_{-1}\rangle_{c_2}. \quad (12)$$

According to eq. (3), after measuring the c_2 qubit in X basis, if the auxiliary photon is flipped to $\frac{1}{\sqrt{2}}(|L\rangle - |R\rangle)$, state $|\Phi_1\rangle \otimes |\Phi\rangle_{c_2}$ will collapse to the maximally entangle W state

$$|\Psi\rangle'' = \frac{1}{\sqrt{3}}(|g_{+1}\rangle_{a_1}|g_{+1}\rangle_{b_1}|g_{-1}\rangle_{c_1} + |g_{-1}\rangle_{a_1}|g_{+1}\rangle_{b_1}|g_{+1}\rangle_{c_1} + |g_{+1}\rangle_{a_1}|g_{-1}\rangle_{b_1}|g_{+1}\rangle_{c_1}), \quad (13)$$

with the success probability

$$P^2 = \frac{3|\beta|^2|\delta|^2}{(|\delta|^2+|\beta|^2)(|\delta|^2+2|\beta|^2)}. \quad (14)$$

So far, we have briefly explained the basic principle of the ECP. Interestingly, different from the ECP with linear optics, this ECP can be repeated to obtain a high success probability. For example, in the first step performed by Alice, he only picks up the cases that the single photon is flipped to the $\frac{1}{\sqrt{2}}(|L\rangle - |R\rangle)$. Certainly, the single photon does not change with some probability. In this way, from eq. (6), by measuring the single photon and the auxiliary N-V center qubit a_2, Alice will obtain

$$|\Psi_1\rangle' = \frac{\alpha^2}{\sqrt{\alpha^2+\beta^2}}|g_{-1}\rangle_{a_1}|g_{+1}\rangle_{b_1}|g_{+1}\rangle_{c_1} + \frac{\beta^2}{\sqrt{\alpha^2+\beta^2}}|g_{+1}\rangle_{a_1}|g_{-1}\rangle_{b1}|g_{+1}\rangle_{c1} + \frac{\beta\delta}{\sqrt{\alpha^2+\beta^2}}|g_{+1}\rangle_{a_1}|g_{+1}\rangle_{b_1}|g_{-1}\rangle_{c_1}. \quad (15)$$

Compared $|\Psi_1\rangle'$ with the initial less-entangled W state shown in eq. (4), it can be found that $|\Psi_1\rangle'$ has the same form with the initial less-entangled W state. Therefore, it can also be reconcentrated with the help of another single photon and the auxiliary N-V center qubit in the second round. Certainly, Alice should re-prepare the auxiliary solid qubit a_2. The similar way can also be performed by Charlie, if the polarization of his auxiliary photon does not change, it will make the state in eq. (12) become

$$|\Psi_2\rangle' = \frac{\delta}{\sqrt{\delta^2+2\beta^2}}\frac{\delta}{\sqrt{\gamma^2+\beta^2}}|g_{+1}\rangle_{a_1}|g_{+1}\rangle_{b_1}|g_{-1}\rangle_{c_1} + \frac{\beta}{\sqrt{\delta^2+2\beta^2}}\frac{\beta}{\sqrt{\gamma^2+\beta^2}}|g_{-1}\rangle_{a_1}|g_{+1}\rangle_{b_1}|g_{+1}\rangle_{c_1}$$
$$+\frac{\beta}{\sqrt{\delta^2+2\beta^2}}\frac{\beta}{\sqrt{\gamma^2+\beta^2}}|g_{+1}\rangle_{a_1}|g_{-1}\rangle_{b_1}|g_{+1}\rangle_{c_1}. \quad (16)$$

By both Alice and Charlie repeating this ECP, they can obtain a high success probability.

3 Discussion and summary

So far, we have fully explained this ECP. We can calculate the total success probability by repeating this ECP. During the practical experiment, we should consider the photon loss, which may be the main obstacle in realistic experiment. It may occur due to the fiber absorption, the coupling of the fiber and the cavity. Certainly, the imperfect detection can also lead to the photon loss. If they can not detect the photon, it is a failure. Then they should restart the protocol. Therefore, the imperfect detection will greatly affect the total success probability. Fortunately, according to eq. (3), it does not affect the fidelity of the entangled state, for the state N-V center does not change. Suppose that the efficiency of the single-photon detector is $\eta_d = 0.8$, the transmission efficiency of each photon through the N-V center is $\eta_T = 0.95$ and the efficiency of coupling and transmission of each photon through the single-mode fiber is $\eta_f = 0.9$. We can estimate the total detection success probability of each concentration round as

$$P_t = \eta_d\eta_f\eta_T^2. \quad (17)$$

In the first step, we calculate the success probability in each iterated round as

$$P_1^1 = \frac{|\alpha|^2(|\delta|^2+2|\beta|^2)}{|\alpha|^2+|\beta|^2}P_t,$$
$$P_2^1 = \frac{|\alpha|^4(|\beta|^2|\delta|^2+2|\beta|^4)}{(|\alpha|^4+|\beta|^4)(|\alpha|^2+|\beta|^2)}P_t^2,$$
$$P_3^1 = \frac{|\alpha|^8(|\beta|^6|\delta|^2+2|\beta|^8)}{(|\alpha|^8+|\beta|^8)(|\alpha|^4+|\beta|^4)(|\alpha|^2+|\beta|^2)}P_t^3,$$
$$\cdots$$
$$P_N^1 = \frac{|\alpha|^{2^N}(|\beta|^{2^N-2}|\delta|^2+2|\beta|^{2^N})}{(|\alpha|^{2^N}+|\beta|^{2^N})(|\alpha|^{2^{N-1}}+|\beta|^{2^{N-1}})\cdots(|\alpha|^2+|\beta|^2)} \times P_t^N. \quad (18)$$

Here the subscript "1", "2", $\cdots$ "N" is the number of the concentration round. The superscript "1" is the first step performed by Alice.

Following the same principle, in the second step performed by Charlie, the success probability in each iterated round is

$$P_1^2 = \frac{3|\beta|^2|\delta|^2}{(|\delta|^2+|\beta|^2)(|\delta|^2+2|\beta|^2)}P_t,$$
$$P_2^2 = \frac{3|\beta|^4|\delta|^4}{(|\delta|^2+2|\beta|^2)(|\delta|^4+|\beta|^4)(|\delta|^2+|\beta|^2)}P_t^2,$$
$$P_3^2 = \frac{3|\beta|^8|\delta|^8}{(|\delta|^2+2|\beta|^2)(|\delta|^8+|\beta|^8)(|\delta|^4+|\beta|^4)(|\delta|^2+|\beta|^2)} \times P_t^3,$$

$$\cdots$$

$$P_M^2 = \frac{3|\beta|^{2^M}|\delta|^{2^M}}{(|\delta|^{2^M}+|\beta|^{2^M})(|\delta|^{2^{M-1}}+|\beta|^{2^{M-1}})\cdots(|\delta|^2+|\beta|^2)} \times \frac{1}{(|\delta|^2+2|\beta|^2)} P_{\mathrm{t}}^M. \quad (19)$$

Therefore, the total success probability can be described as

$$P_{\mathrm{total}} = \sum_{N=1}^{\infty} P_N^1 \sum_{M=1}^{\infty} P_M^2. \quad (20)$$

In Figure 3, we calculate the practical success probability with different initial coefficient α. We let $\beta = \frac{1}{\sqrt{3}}$ and change α from 0 to $\sqrt{\frac{2}{3}}$. Curve A denotes that both Alice and Charlie repeat their protocol with $N = M = 3$, and Curve B denotes that Alice and Charlie does not repeat their protocol with $N = M = 1$. In Figure 3, the total success probability in Curve A is greater than that in Curve B with the same α. When $\alpha \in \left\{0, \frac{1}{\sqrt{3}}\right\}$, the success probability in both curves increases, while it decreases when $\alpha \in \left\{\frac{1}{\sqrt{3}}, \frac{2}{\sqrt{3}}\right\}$. They can obtain a higher success probability if the ECP is repeated. The max value of P_{total} in Curve B is $P_{\mathrm{total}} \approx 0.10$, while it can reach $P_{\mathrm{total}} \approx 0.22$ in Curve A. Finally, let us discuss the practical experiment with such devices. Over past years, a variety of cavity QED systems have been studied for N-V centers. It is shown that the coupling strength of the N-V center to an optical resonator can reach the order of hundreds of megahertz. Certainly, there are also other imperfect control during the practical operation, such as the Debye-Waller factor. Current experiment showed that with the cavity of a low-Q factor $Q \sim 10^4$, the coupling of a N-V center and a GaP microdisk has reached the relevant parameters $\Omega/2\pi = 0.6$ GHz, $\kappa/2\pi = 26$ GHz [74]. The large coupling between N-V centers and photonic crystal nanocavities has been realized [75]. Moreover, as shown in [76], the dephasing time of the N-V center is about 2 ms in an isotopically pure diamond. It provides us enough time to complete the operation for the ECP.

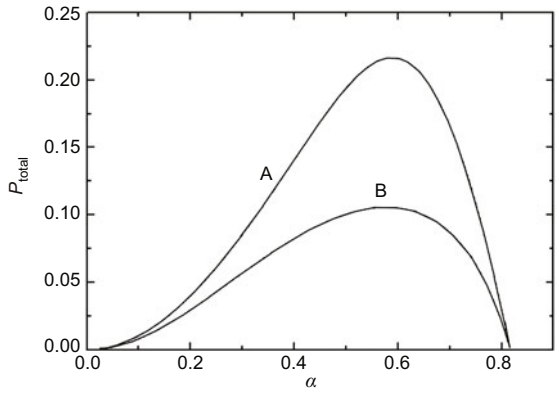

Figure 3 The total success probability P_{total} for getting a maximally entangled W state is altered with the α. We let $\beta = \frac{1}{\sqrt{3}}$ and change α from 0 to $\sqrt{\frac{2}{3}}$. Curve B is the success probability for only performing the ECP for one time. Curve A is the success probability for both Alice and Charlie repeating this ECP for three times. It is shown that the P_{total} increases greatly.

In conclusion, we have described an ECP for multi-particle W state for separated N-V centers via coupling to microtoroidal resonators. With the help of single photons and two single auxiliary N-V centers in microcavity, we can obtain the maximally entangled W state with some success probability. During the whole protocol, we do not need to destroy the solid qubits instead of consuming some single photons, which makes it more feasible. Moreover, our ECP can be repeated to obtain a higher success probability even in an imperfect and practical experiment.

This work was supported by the National Natural Science Foundation of China (11104159), Open Research Fund Program of the State Key Laboratory of Low-Dimensional Quantum Physics Scientific, Tsinghua University, Open Research Fund Program of National Laboratory of Solid State Microstructures, Nanjing University (M25022), the Project Funded by the Priority, University Natural Science Research Project of Jiangsu Province (13KJB140010), Academic Program Development of Jiangsu Higher Education Institutions and the Open Research Fund of Key Laboratory of Broadband Wireless Communication and Sensor Network Technology, Nanjing University of Posts and Telecommunications, Ministry of Education (NYKL201303).

1 Gisin N, Ribordy G, Tittel W, et al. Quantum cryptography. Rev Mod Phys, 2002, 74: 145–195
2 Ekert A K. Quantum cryptography based on Bells theorem. Phys Rev Lett, 1991, 67: 661–663
3 Deng F G, Long G L. Controlled order rearrangement encryption for quantum key distribution. Phys Rev A, 2003, 68: 042315
4 Li X H, Deng F G, Zhou H Y. Efficient quantum key distribution over a collective noise channel. Phys Rev A, 2008, 78: 022321
5 Yan T, Yan F L. Quantum key distribution using four-level particles. Chin Sci Bull, 2011, 56: 24–28
6 Bennett C H, Brassard G, Crepeau C, et al. Teleporting an unknown quantum state via dual classical and Einstein-Podolsky-Rosen channels. Phys Rev Lett, 1993, 70: 1895–1899
7 Yan F L, Yan T. Probabilistic teleportation via a non-maximally entangled GHZ state. Chin Sci Bull, 2010, 55: 902–906
8 Deng F G, Li C Y, Li Y S, et al. Symmetric multiparty-controlled teleportation of an arbitrary two-particle entanglement. Phys Rev A, 2005, 72: 022338
9 Bennett C H, Wiesner S J. Communication via one- and two-particle operators on Einstein-Podolsky-Rosen states. Phys Rev Lett, 1992, 69: 2881–2884
10 Zhang J F, Xie J Y, Wang C A, et al. Implementation of a multiple round quantum dense coding using nuclear magnetic resonance. Sci China Ser G Phys Mech Astro, 2005, 48: 706–715
11 Li C Y, Li X H, Deng F G, et al. Complete multiple round quantum dense coding with quantum logical network. Chin Sci Bull, 2007, 52: 1162–1165
12 Hillery M, Bužek V, Berthiaume A. Quantum secret sharing. Phys Rev A, 1999, 59: 1829–1834
13 Karlsson A, Koashi M, Imoto N. Quantum entanglement for secret sharing and secret splitting. Phys Rev A, 1999, 59: 162–168
14 Xiao L, Long G L, Deng F G, et al. Efficient multiparty quantum-secret-sharing schemes. Phys Rev A, 2004, 69: 052307
15 Cleve R, Gottesman D, Lo H K. How to share a quantum secret. Phys Rev Lett, 1999, 83: 648–651

16 Lance A M, Symul T, Bowen W P, et al. Tripartite quantum state sharing. Phys Rev Lett, 2004, 92: 177903
17 Deng F G, Li X H, Li C Y, et al. Multiparty quantum-state sharing of an arbitrary two-particle state with Einstein-Podolsky-Rosen pairs. Phys Rev A, 2005, 72: 044301
18 Long G L, Liu X S. Theoretically efficient high-capacity quantum-key-distribution scheme. Phys Rev A, 2002, 65: 032302
19 Deng F G, Long G L, Liu X S. Two-step quantum direct communication protocol using the Einstein-Podolsky-Rosen pair block. Phys Rev A, 2003, 68: 042317
20 Wang C, Deng F G, Li Y S, et al. Robustness of differential-phase-shift quantum key distribution against photon-number-splitting attack. Phys Rev A, 2005, 71: 042305
21 Gu B, Huang Y G, Fang X, et al. A two-step quantum secure direct communication protocol with hyperentanglement. Chin Phys B, 2011, 20: 100309
22 Li X H, Duan X J, Sheng Y B, et al. Faithful quantum entanglement sharing based on linear optics with additional qubits. Chin Phys B, 2009, 18: 3710–3713
23 Liu X S, Long G L, Tong D M, et al. General scheme for superdense coding between multiparties. Phys Rev A, 2002, 65: 022304
24 Deng F G, Long G L. Secure direct communication with a quantum one-time pad. Phys Rev A, 2004, 69: 052319
25 Long G L, Deng F G, Wang C, et al. Quantum secure direct communication and deterministic secure quantum communication. Front Phys China, 2007, 2: 251–272
26 Gu B, Li C Q, Xu F, et al. High-capacity three-party quantum secret sharing with superdense coding. Chin Phys B, 2009, 18: 4690–4694
27 Gu B, Li C Q, Chen Y L. Multiparty quantum secret conference based on quantum encryption with pure entangled states. Chin Phys B, 2009, 18: 2137–2142
28 Bennett C H, Brassard G, Popescu S, et al. Purification of noisy entanglement and faithful teleportation via noisy channels. Phys Rev Lett, 1996, 76: 722–725
29 Sheng Y B, Deng F G, Zhou H Y. Efficient polarization-entanglement purification based on parametric down-conversion sources with cross-Kerr nonlinearity. Phys Rev A, 2008, 77: 042308
30 Sheng Y B, Deng F G. Deterministic entanglement purification and complete nonlocal Bell-state analysis with hyperentanglement. Phys Rev A, 2010, 81: 032307
31 Sheng Y B, Deng F G. One-step deterministic polarization-entanglement purification using spatial entanglement. Phys Rev A, 2010, 82: 044305
32 Cao C, Wang C, He L Y, et al. Atomic entanglement purification and concentration using coherent state input-output process in low-Q cavity QED regime. Opt Express, 2013, 21: 4093–4105
33 Deng F G. Efficient multipartite entanglement purification with the entanglement link from a subspace. Phys Rev A, 2011, 84: 052312
34 Deng F G. One-step error correction for multipartite polarization entanglement. Phys Rev A, 2011, 83: 062316
35 Li X H. Deterministic polarization-entanglement purification using spatial entanglement. Phys Rev A, 2010, 82: 044304
36 Bennett C H, Bernstein H J, Popescu S, et al. Concentrating partial entanglement by local operations. Phys Rev A, 1996, 53: 2046–2052
37 Shi B S, Jiang Y K, Guo G C. Optimal entanglement purification via entanglement swapping. Phys Rev A, 2000, 62: 054301
38 Zhao Z, Pan J W, Zhan M S. Practical scheme for entanglement concentration. Phys Rev A, 2001, 64: 014301
39 Yamamoto T, Koashi M, Imoto N. Concentration and purification scheme for two partially entangled photon pairs. Phys Rev A, 2001, 64: 012304
40 Sheng Y B, Deng F G, Zhou H Y. Nonlocal entanglement concentration scheme for partially entangled multipartite systems with nonlinear optics. Phys Rev A, 2008, 77: 062325
41 Sheng Y B, Zhou L, Zhao S M, et al. Efficient single-photon-assisted entanglement concentration for partially entangled photon pairs. Phys Rev A, 2012, 85: 012307
42 Sheng Y B, Zhou L, Zhao S M. Efficient two-step entanglement concentration for arbitrary W states. Phys Rev A, 2012, 85: 044302
43 Du F F, Li T, Ren B C, et al. Single-photon-assisted entanglement concentration of a multi-photon system in a partially entangled W state with weak cross-Kerr nonlinearity. J Opt Soc Am B, 2012, 29: 1399–1405
44 Gu B. Single-photon-assisted entanglement concentration of partially entangled multiphoton W states with linear optics. J Opt Soc Am B, 2012, 7: 1685–1689
45 Gu B, Duan D H, Xiao S R. Multi-photon entanglement concentration protocol for partially entangled W states with projection measurement. Int J Theor Phys, 2012, 51: 2966–2973
46 Wang H F, Zhang S, Yeon K H. Linear-optics-based entanglement concentration of unknown partially entangled three photon W states. J Opt Soc Am B, 2010, 27: 2159–2164
47 Xiong W, Ye L. Schemes for entanglement concentration of two unknown partially entangled states with cross-Kerr nonlinearity. J Opt Soc Am B, 2011, 28: 2030–2037
48 Zhou L, Sheng Y B, Cheng W W, et al. Efficient entanglement concentration for arbitrary single-photon multimode W state. J Opt Soc Am B, 2013, 30: 71–78
49 Zhou L, Sheng Y B, Cheng W W, et al. Efficient entanglement concentration for arbitrary less-entangled NOON states. Quant Inf Process, 2013, 12: 1307–1320
50 Deng F G. Optimal nonlocal multipartite entanglement concentration based on projection measurements. Phys Rev A, 2012, 85: 022311
51 Sheng Y B, Deng F G, Zhou H Y. Single-photon entanglement concentration for long-distance quantum communication. Quant Inf Comput, 2010, 10: 272–281
52 Zhang C W. Entanglement concentration of individual photon pairs via linear optical logic. Quant Inf Comput, 2004, 4: 196–200
53 Zhou L, Sheng Y B, Zhao S M. Optimal entanglement concentration for three-photon W states with parity check measurement. Chin Phys B, 2013, 22: 020307
54 Wang C. Efficient entanglement concentration for partially entangled electrons using a quantum-dot and microcavity coupled system. Phys Rev A, 2012, 86: 012323
55 Sheng Y B, Zhou L, Wang L, et al. Efficient entanglement concentration for quantum dot and optical microcavities systems. Quant Inf Process, 2013, 12: 1885–1895
56 Sheng Y B, Deng F G, Zhou H Y. Efficient polarization entanglement concentration for electrons with charge detection. Phys Lett A, 2009, 373: 1823–1825
57 Zhou L. Efficient entanglement concentration for electron-spin W state with the charge detection. Quant Inf Process, 2013, 12: 2087–2101
58 Ren B C, Hua M, Li T, et al. Multipartite entanglement concentration of electron-spin states with CNOT gates. Chin Phys B, 2012, 21: 090303
59 Peng Z H, Zou J, Liu X J, et al. Atomic and photonic entanglement concentration via photonic Faraday. Phys Rev A, 2012, 86: 034305
60 Zhang L H, Yang M, Cao Z L. Entanglement concentration for unknown W class states. Physica A, 2007, 374: 611–616
61 Wang H F, Zhang S, Yeon K H. Linear optical scheme for entanglement concentration of two partially entangled three-photon W states. Eur Phys J D, 2010, 56: 271–275
62 Wang H F, Sun L L, Zhang S, et al. Scheme for entanglement concentration of unkonwn partially entangled three-atom W states in cavity QED. Quan Inf Process, 2012, 11: 431–441
63 Cao Z L, Yang M. Entanglement distillation for three particle W class

states. J Phys B, 2003, 36: 4245–4253
64 Sheng Y B, Zhou L. Efficient W state entanglement concentration using quantum-dot and optical microcavities. J Opt Soc Am B, 2013, 30: 678–686
65 He L Y, Cao C, Wang C. Entanglement concentration for multi-particle partially entangled W state using nitrogen vacancy center and microtoroidal resonator system. Opt Commun, 2013, 298: 260–266
66 Gaebel T, Domhan M, Popa I, et al. Room-temperature coherent coupling of single spins in diamond. Nat Phys, 2006, 2: 408–413
67 Togan E, Chu Y, Trifonov A S, et al. Quantum entanglement between an optical photon and a solid-state spin qubit. Nature, 2010, 466: 730–734
68 Yang W L, Xu Z Y, Feng M, et al. Entanglement of separate nitrogen-vacancy centers coupled to a whispering-gallery mode cavity. New J Phys, 2010, 12: 113039
69 Yang W L, Yin Z Q, Hu Y, et al. High-fidelity quantum memory using nitrogen-vacancy center ensemble for hybrid quantum computation. Phys Rev A, 2011, 84: 010301(R)
70 Chen Q, Yang W L, Feng M, et al. Entangling separate nitrogen-vacancy centers in a scalable fashion via coupling to microtoroidal resonators. Phys Rev A, 2011, 83: 054305
71 Li P B, Gao S Y, Li F L. Quantum-information transfer with nitrogen-vacancy centers coupled to a whispering-gallery microresonator. Phys Rev A, 2011, 83: 054306
72 Jiang L, Hodges J S, Maze J R, et al. Repetitive readout of a single electron spin via quantum logic with nuclear spin ancillae. Science, 2009, 326: 267–272
73 Wang C, Zhang Y, Jin G S, et al. Efficient entanglement purification of separate nitrogen-vacancy centers via coupling to microtoroidal resonators. J Opt Soc Am B, 2012, 12: 3349–3354
74 Barclay P E, Fu K M, Santori C, et al. Chip-based microcavities coupled to nitrogen-vacancy centers in single crystal diamond. Appl Phys Lett, 2009, 95: 191115
75 Barclay P E, Santori C C, Fu K M, et al. Coherent interference effects in a nano-assembled diamond NV center cavity-QED system. Opt Express, 2009, 17: 8081–8097
76 Balasubramanian G, Neumann P, Twitchen D, et al. Ultralong spin coherence time in isotopically engineered diamond. Nat Mater, 2009, 8: 383–387